JOURNAL OF GUIDANCE, CONTROL, AND DYNAMICS
Vol. 27, No. 5, September–October 2004

Method for Determination of Nonlinear Attainable Moment Sets

Michael A. Bolender* and David B. Doman†
U.S. Air Force Research Laboratory, Wright–Patterson Air Force Base, Ohio 45433

A method for generating attainable moment sets for left–right pairs of nonlinear control effectors on aircraft is presented. It is shown that the determination of the attainable moment set boundary can be posed as a constrained, nonlinear optimization problem. The first-order necessary conditions for a point to be on the boundary are simply the Kuhn–Tucker first-order necessary conditions. An algorithm is given where the Kuhn–Tucker points for a given point in the pitch–roll plane are constructed for each control effector configuration that forms a candidate boundary. The Kuhn–Tucker points are then checked for feasibility, and the points on the boundary are those that produce extremal values of the objective function. The nonlinear attainable moment set boundary is used to determine feasibility of moment commands generated by the flight control system. Infeasible commands are clipped to the boundary of the attainable moment set. If a commanded moment is feasible, a constrained optimization problem is solved for the control surface deflections.

Introduction

MODERN aerospace vehicles are being designed with a mix of conventional and unconventional control effectors. To take full advantage of the effector suite, reconfigurable flight control systems and control allocation algorithms are being developed to maintain performance and robustness in the presence of control effector failures. One such application is the use of a dynamic-inversion control law for the next generation of reusable launch vehicles.[1] In addition, Buffington has demonstrated the application of a dynamic-inversion control law and a control allocation algorithm to a tailless fighter application.[2] Tailless aircraft have reduced directional stability due to the lack of a vertical tail and rudder for directional control. Ailerons or spoilers are examples of conventional control surfaces that can be used to provide directional control; however, these control effectors lack the control authority that a rudder would have, requiring that a mix of control effectors be used to generate the appropriate moments.

Numerous linear control allocation and control effector mixing algorithms have been developed over the past decade, and excellent survey papers have been written that point out the strengths and weaknesses of the existing approaches. Bodson[3] compared constrained, numerical-based optimization methods to determine their feasibility for use in a real-time flight control system. Page and Steinberg[4,5] have performed extensive simulation studies on the open- and closed-loop performance of the most common linear control allocation algorithms. These surveys focused on the state-of-the-art control allocation algorithms, all of which are control allocation methods that assume a linear relationship between the control effectors and the control moments. Although this assumption may be valid locally for many of the control surfaces found on aircraft, there are exceptions.

One particular case where the assumption of linearity can result in incorrect control surface deflections involves the use of left–right aerodynamic control surfaces on aircraft. Examples of left–right aerodynamic surfaces include left–right elevators and left–right ailerons. These types of surfaces, when actuated independently, generally produce pitching, rolling, and yawing moments. Whereas these surfaces normally produce pitching and rolling moments that are locally linear in control surface deflection, they can have a highly nonlinear contribution to the yawing moment. This is especially true when parasitic drag dominates induced drag effects at low angles of attack.

In particular, these surfaces can generate yawing moments that are of the same sign whether they are deflected up or down. This is because they generate a drag force on the side of the vehicle on which they are located regardless of whether they are deflected in the positive or negative direction. The yawing moments generated by these effectors are usually small when compared to a primary yaw-axis effector such as rudder; however, their effects can become significant when a failure requires that these effectors be used for yaw control.

This particular nonlinearity is important because it is common on many aircraft; therefore, it used as motivation and serves as an example for the method of generating the nonlinear attainable moment set (AMS) that is presented in this paper. We focus on the computation of the AMS and its application in a flight control system. The advantage of the AMS is that it allows us to determine easily the feasibility of a commanded moment. If the commanded moment lies outside the AMS, then the moment is clipped to the boundary. If the commanded moment lies within the interior, then an optimization problem can be solved as opposed to a nonlinear program with bounds on the decision variables. Also, determining the attainable moment set allows us to estimate the maximum capabilities of the aircraft for more accurate trajectory planning. The nonlinear control allocation problem is of interest especially when there are control effector failures, in as much as a more accurate representation of the aircraft's capabilities will enable the vehicle to be recovered from a wider range of failure scenarios than can be accomplished using linear allocation methods.

Attainable Moment Set for a Single Left–Right Pair

Durham[6,7] developed and subsequently refined methods for determining an attainable moment set for effectors that generate moments $\boldsymbol{M}$ that are linear combinations $\boldsymbol{M} = \boldsymbol{B}\boldsymbol{\delta}$ of the effector positions $\boldsymbol{\delta}$, subject only to constraints on those positions $\boldsymbol{\delta} = \{\boldsymbol{\delta} \,|\, \boldsymbol{\delta}_{\min} \leq \boldsymbol{\delta} \leq \boldsymbol{\delta}_{\max}\}$. There are two approaches regarding the determination of the control effectiveness matrix. The first approach is based on a finite difference approximation about some given effector position to determine a local slope. The second approach is to calculate a least-squares fit over the entire deflection range to determine the slope of the line. We will take the latter approach in determining the nonlinear AMS to ensure that nonlinearities such as slope reversals are modeled. The method used to determine an attainable moment set for an overactuated linear system with position constraints involves constructing a polyhedron in moment

Received 26 December 2002; revision received 6 November 2003; accepted for publication 8 March 2004.

*Visiting Scientist, Control Theory and Optimization Branch. Senior Member AIAA.

†Senior Aerospace Engineer, Control Theory and Optimization Branch. Senior Member AIAA.

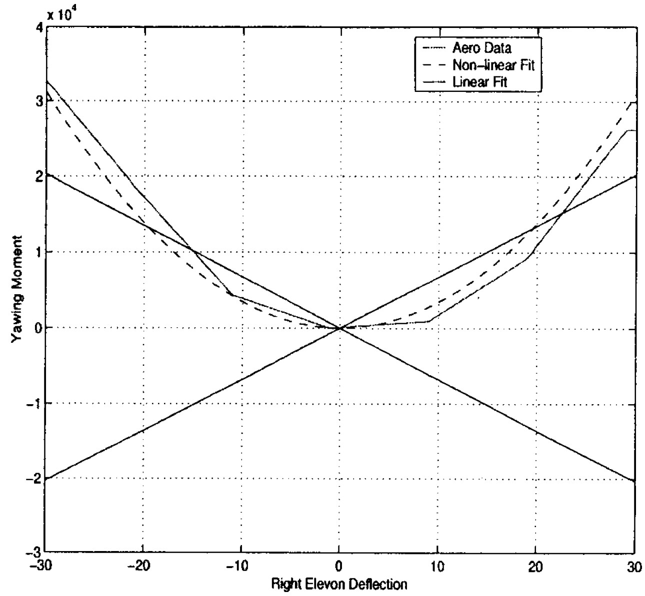

Fig. 1 Yawing moment due to right elevon deflection.

space. Potential vertices are constructed by locking all control effectors at their extreme positions in all possible combinations while allowing two effectors to traverse the range of their possible positions. Durham's algorithm connected the vertices to form potential boundary facets and determined which facets were on the boundary of the AMS.

Left–right (LR) pairs of effectors such as ailerons, elevators, and flaps generate nonlinear contributions to the vehicle yawing moment. Figure 1 shows the yawing moment that is generated by deflecting the right elevon of a particular lifting body vehicle. One can see that a parabolic fit provides an adequate approximation of the original data. Generation of linear fits to these data for use in a conventional control allocator that assumes a linear relationship between the moments and control effector deflections is problematic. This is because lines fitted using either negative deflection or positive deflection data result in lines with slopes of opposite signs. Furthermore, because no single line can accurately model the data and no matter which line is selected, the sign of the yawing moment estimate will be incorrect half of the time.

Here we examine a case where an LR pair of elevons exerts a yawing moment N that is proportional to the square of deflection, and the rolling and pitching moments L and M are linear functions of deflection, that is,

$$L = L_{\delta_1}\delta_1 + L_{\delta_2}\delta_2 \tag{1}$$

$$M = M_{\delta_1}\delta_1 + M_{\delta_2}\delta_2 \tag{2}$$

$$N = N_{\delta_1^2}\delta_1^2 + N_{\delta_2^2}\delta_2^2 \tag{3}$$

From the curve fits to aerodynamic data for a lifting body model at a subsonic, low angle-of-attack flight condition, we select $N_{\delta_1^2} = -N_{\delta_2^2} = 34$ ft · lb/deg^2 and $L_{\delta_1} = -L_{\delta_2} = -4610$ ft · lb/deg, and $M_{\delta_1} = M_{\delta_2} = -2489$ ft · lb/deg. In addition, we impose the following position constraints such that $-30 \le \delta_i \le 30$ deg. The AMS for this single LR pair is shown in Fig. 2, and this AMS is generated by holding each control surface at a fixed deflection while allowing the other surface to vary over its range of possible values. Note in particular that the shape of the AMS is a hyperbolic paraboloid. This saddle shape is a characteristic of LR control effector pairs on any aircraft operating at flight conditions where parasitic drag effects dominate induced drag effects, that is, at low angles of attack.

If one uses a linear approximation to describe the relationship between yawing moment and LR elevator deflection, one will find that the AMS becomes a plane, as shown in Fig. 3. For the linear approximation, we fit data over half of the range of deflections to

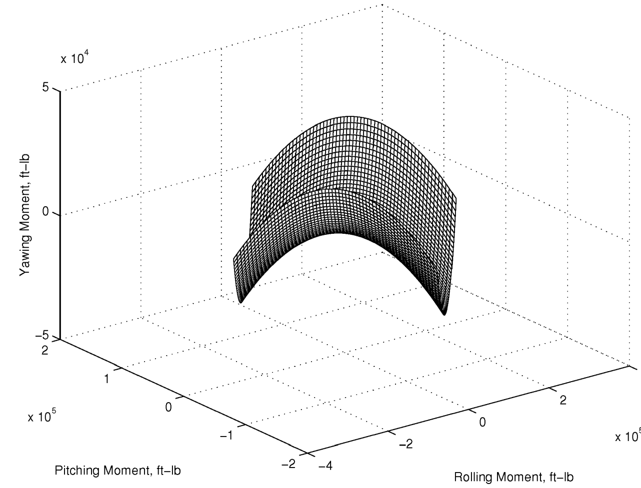

Fig. 2 Nonlinear AMS and lines of constant deflection in moment space.

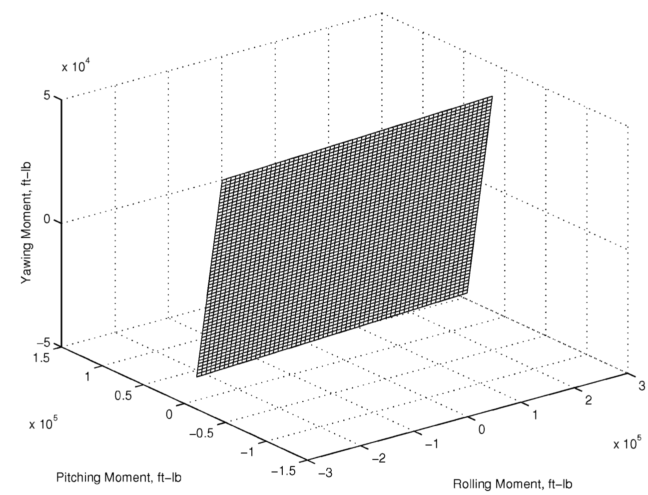

Fig. 3 Linear AMS for a single LR pair.

obtain $N_{\delta_1} = -N_{\delta_2} = \pm 676$ ft · lb/deg. The sign ambiguity results from the yawing moment derivatives' dependency on the sign of the deflections; either choice of sign will only yield a yawing moment with the correct sign over half of the deflection range. The AMS for the linear case shows that a control allocator that incorrectly assumes a linear relationship between the yawing moment and the effector deflections will be constrained to rolling, pitching, and yawing moments that lie on a plane in moment space. The grid lines are lines of constant effector deflection that inturn define the proper blend of effectors required to achieve a particular rolling, pitching, and yawing moment that lies on the AMS.

Determination of the Composite AMS for Multiple Effectors

The generation of an AMS for a single LR pair is relatively straightforward. Here we explore methods for generating the AMS for multiple LR effector pairs. To consider how this might be accomplished, we consider the rolling, pitching, and yawing moments that can be generated by two LR effector pairs of the form

$$L = L_{\delta_1}\delta_1 + L_{\delta_2}\delta_2 + L_{\delta_3}\delta_3 + L_{\delta_4}\delta_4 \tag{4}$$

$$M = M_{\delta_1}\delta_1 + M_{\delta_2}\delta_2 + M_{\delta_3}\delta_3 + M_{\delta_4}\delta_4 \tag{5}$$

$$N = N_{\delta_1^2}\delta_1^2 + N_{\delta_2^2}\delta_2^2 + N_{\delta_3^2}\delta_3^2 + N_{\delta_4^2}\delta_4^2 \tag{6}$$

Because there is no aerodynamic coupling between the control effectors, Eqs. (4–6) can be written as follows:

$$L = L_{12} + L_{34} \tag{7}$$

$$M = M_{12} + M_{34} \tag{8}$$

$$N = N_{12} + N_{34} \tag{9}$$

Generating an AMS for one pair of effectors is relatively simple. This leads one to ask whether or not there exists a method for generating the AMS for multiple LR pairs through some combination of the attainable moment sets for single LR pairs. For the class of nonlinearity being considered, the yawing moment is a quadratic function of displacement and the rolling and pitching moments are linear functions of displacement. The composite AMS may be generated by sweeping the AMS for the first LR pair over the AMS of the second LR pair. This approach is sufficient for generating every attainable moment; however, a criterion is needed to determine the boundary of the AMS. We will briefly discuss the possibility of using swept volume theory to construct the AMS; however, this method only determines those surfaces that are candidates to lie on the boundary. The problem of boundary determination typically requires exhaustive searches over each candidate surface.[8,9] We then present a method that extends the work of Doman and Sparks[10] to three-dimensional volumes.

One possible approach to generating the nonlinear attainable moment set is through the application of swept volume theory. The application of swept volume theory to the determination of the attainable moment set will be briefly discussed here; however, the reader is referred to Bolender and Doman[11] for more detail on the computational procedure as applied to the determination of candidate surfaces for the nonlinear AMS. A swept volume is defined by Adbel-Malek et al.[12] as "the volume generated by the motion of an arbitrary object along an arbitrary path (or even a surface) possibly with arbitrary rotations." Our interest in swept volume theory was motivated by the observation that the AMS is generated by the sweeping of one surface over another.

The primary strength of swept volume theory lies in its ability to generate, using the Jacobian rank deficiency criteria, surfaces that are candidates for the boundary of the AMS. In short, the method takes into consideration all cases where the Jacobian formed from Eqs. (4–6) becomes singular. From these conditions, one is able to determine easily a set of effector positions that generate candidate surfaces for the AMS boundary. An additional set of candidate surfaces is constructed by fixing all but two control effectors at their limits and letting the remaining two free control effectors vary continuously between their upper and lower limits. This is done for all possible effector combinations. Once the set of candidate surfaces is completed, the next step is then to determine if some patch of a candidate surface lies on the AMS boundary. Currently, there is no widely accepted boundary determination method, and this is an area of active research within the swept volume community. However, two of the more common approaches to boundary determination are the perturbation technique[8] and a technique that uses differential geometry.[9] The downside of these techniques is that they require an exhaustive search over a grid of points on each candidate surface. These methods are clearly inefficient and not suitable for a flight control application.

Our work with swept volume theory and the recognition of its shortcomings led us to consider alternate approaches for the construction of the AMS volume. We learned from the application of swept volume theory to Eqs. (4–6) that the candidate surfaces are defined by considering all combinations of control effector positions where two effectors are fixed at either an upper or lower bound and the remaining two effectors are allowed to take any admissible value. In addition, we must consider all combinations of effector positions where only one control effector is set at its upper and lower limits while the remaining three effectors are free to vary. This gives us 32 distinct surfaces to consider as candidates for the AMS boundary.

New Method for the Determination of the AMS Volume

As already stated, the composite AMS can be generated by sweeping the AMS for one LR pair over the AMS for the second LR pair. We also know from Ref. 11 the set of control surface deflections that will generate the candidate surfaces for the AMS boundary. However, we still lack a means of determining which patches of the candidate surfaces define the AMS boundary.

Therefore, in this section, we will revisit and extend the approach of Doman and Sparks[10] to the problem of computing the AMS volume in moment space. The theorem developed by Doman and Sparks gives a necessary condition for a point to lie on the composite boundary. When extended to three-dimensional moment space, it will be shown that we are left to solve a constrained optimization problem. It then follows that the Kuhn–Tucker conditions can be used to determine the boundary. Finally, we will discuss an approach for implementing the nonlinear control allocation problem in a flight control system.

Determination of a Two-Dimensional Nonlinear AMS Boundary

To illustrate how the computation of the AMS boundary might be accomplished, we consider the rolling and yawing moments that can be generated by two LR effector pairs as given in Eqs. (4) and (6). For demonstration purposes, let $N_{\delta_1^2} = -N_{\delta_2^2} = 34$ ft · lb/deg^2, $N_{\delta_3^2} = -N_{\delta_4^2} = N_{\delta_1^2}/25$, $L_{\delta_1} = -L_{\delta_2} = -4610$ ft · lb/deg, and $L_{\delta_3} = -L_{\delta_4} = L_{\delta_1}/5$. We take all effector deflection limits to be ± 30 deg. To generate the upper AMS boundaries for the 1–2 effector pair, we set $\delta_3 = \delta_4 = 0$, $\delta_1 = 30$ or $\delta_1 = -30$, and let δ_2 vary continuously between ± 30. The lower boundaries and the boundaries for the 3–4 effector pair can be generated in a similar fashion. To generate the AMS boundary for both of the LR pairs acting together, one may add the AMS of the 3–4 pair to each point on the 1–2 AMS boundary. Figure 4 shows the effect of performing this operation. In principle, the AMS boundary could be generated by exhaustion by moving the origin of the 3–4 AMS boundary to each point on the 1–2 AMS boundary and drawing a composite AMS for the 1–2–3–4 effectors by drawing a curve that touches the extremal points in the roll–yaw plane. Such a procedure would clearly be inefficient.

It is, therefore, natural to ask if there exists a method or condition that relates the AMS of each LR pair considered individually to points on the composite boundary approximated by the outline of Fig. 4. The condition for a point to be on the boundary turns out to be related to the slope of the AMS boundary curves. For convenience, we shall consider the top left quadrant of two boundaries in the roll–yaw plane and denote the boundary curve for the first LR pair $f(x)$ and the boundary curve for the second LR pair $g(x)$ as shown

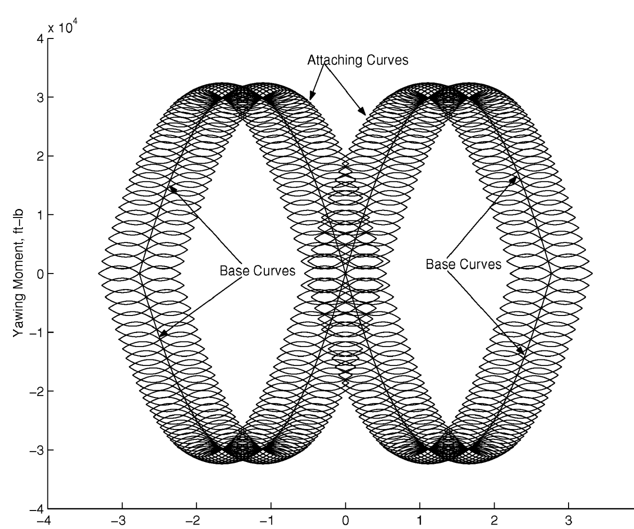

Fig. 4 Generation of AMS by superposition.

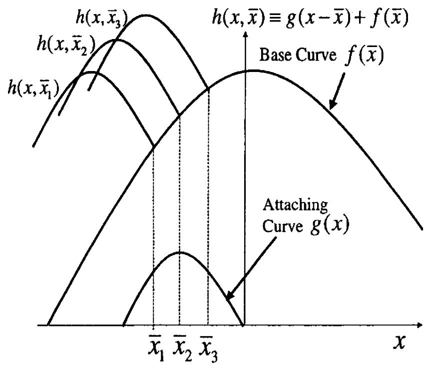

Fig. 5 Generation of the AMS boundary.

in Fig. 5. To generate the composite boundary, one can generate a number of auxiliary functions $h(x,\bar{x}) = g(x-\bar{x}) + f(\bar{x})$ where $[\bar{x}, f(\bar{x})]$ is the point at which the origin of the boundary curve for the second LR pair attaches to the boundary curve for the first LR pair.

Definition 1. An attachment point to $f(x)$ is a point $P[\bar{x}, f(\bar{x})]$ to which the origin of a curve $g(x)$ is translated for the purpose of calculating values of a new function that is composed of the two original functions $h(x,\bar{x}) = g(x-\bar{x}) + f(\bar{x})$.

Hence, $h(x,\bar{x})$ shifts the origin of the original curve $g(x)$ to a point on $f(x)$ at $x = \bar{x}$. We define points on the composite boundary as those that produce maximum or minimum values of $h(x,\bar{x})$ as $\bar{x}$ is varied over its range of physically realizable values.

Definition 2. The composite boundary $b(x)$ generated from all physically realizable values of $h(x,\bar{x}) = g(x-\bar{x}) + f(\bar{x})$ is defined as the set of extremal values of $h(x,\bar{x})$ for $\{\bar{x} \in \mathbb{R}^n | x_{\min_f} \leq \bar{x} \leq x_{\max_f}\}$ and $\{x \in \mathbb{R}^n | x_{\min_f} + x_{\min_g} \leq x \leq x_{\max_f} + x_{\max_g}\}$ where $x_{\min_f}$, $x_{\min_g}$ and $x_{\max_f}$, $x_{\max_g}$ are the minimum and maximum values of x and $\bar{x}$ for which $f(\bar{x})$ and $g(x)$ physically exist.

The theorem states a necessary condition for a point to lie on the composite boundary.

Theorem. If $f(x)$ and $g(x)$ are C^1 with monotonic slopes and $h(x,\bar{x}) = g(x-\bar{x}) + f(\bar{x})$, then for any $x \in \{x \in \mathbb{R}^n | x_{\min_g} \leq (x - \bar{x}^*) \leq x_{\max_g}\}$ a point on the composite boundary, $P[x, h(x, \bar{x}^*)]$ satisfies the following condition:

$$\left.\frac{\partial}{\partial(x-\bar{x})} g(x-\bar{x})\right|_{\bar{x}=\bar{x}^*} = \left.\frac{\partial}{\partial \bar{x}} f(\bar{x})\right|_{\bar{x}=\bar{x}^*} \tag{10}$$

Proof. By definition points on the composite boundary are extremal values of $h(x,\bar{x}) = g(x-\bar{x}) + f(\bar{x})$. It is assumed that $f(x)$ and $g(x)$ have continuous derivatives and that these derivatives are monotonic functions of x. At any given value of x, we are interested in finding an attachment point $P[\bar{x}^*, f(\bar{x}^*)]$ that will result in an extremal value for the composite function $h(x,\bar{x})$. The first-order necessary condition for an extremum of $h(x,\bar{x})$ is

$$\left.\frac{\partial}{\partial \bar{x}} h(x,\bar{x})\right|_{\bar{x}=\bar{x}^*} = 0 \tag{11}$$

With application of the chain rule for derivatives and after routine manipulations, it is easy to verify that Eq. (11) is equivalent to Eq. (10). Because the slopes of $f(x)$ and $g(x)$ are monotonic, there is one and only one value of $\bar{x}$ that satisfies Eq. (10) and this value of $\bar{x}$ is defined as $\bar{x}^*$. □

Note that there is no restriction on the dimension of x. Therefore, for any fixed value of x, we can determine the optimum value of $\bar{x}$ where $g(x-\bar{x})$ attaches to $f(\bar{x})$ to maximize or minimize $h(x,\bar{x})$.

To apply the preceding necessary condition to the determination of the composite AMS, two additional remarks are needed to account for the fact that there are bounds on the variables $x - \bar{x}$ and $\bar{x}$, which in turn bound the range of their respective functions. The remarks are repeated here for completeness.

Remark 1. If $(x - \bar{x}^*) \geq x_{\max_g}$, then the boundary point is given by $P[\bar{x}^* + x_{\max_g}, h(x_{\max_g}, \bar{x}^*)]$.

Remark 2. If $(x - \bar{x}^*) \leq x_{\min_g}$, then the boundary point is given by $P[\bar{x}^* + x_{\min_g}, h(x_{\min_g}, \bar{x}^*)]$.

Doman and Sparks[10] demonstrated that the AMS boundary was determined by the translation of a first AMS due to one LR pair of control effectors over a second AMS due to another LR pair of control effectors (Fig. 5). For this example, the rolling moment was a linear function of the control displacement and the yawing moment was a second-order function of control surface displacement. Note that the result that was achieved was not for the case where the pitching moment was constrained to zero. Instead, their composite AMS was a projection of the AMS volume onto the roll–yaw plane.

Determination of the Three-Dimensional Nonlinear AMS Boundary

The next logical step is to consider the moments about all three axes and to develop a method along the lines of that just presented for the determination of the three-dimensional AMS boundary. In this section, we outline a method to determine the boundary of the AMS when given any feasible point in the L–M plane. For purposes of illustration, we will only consider the case where there are two LR pairs of control effectors. For brevity, we will demonstrate the method only by considering combinations of δ_2 and δ_4 set at their position limits. (An alternate derivation is given in Appendix A that derives the necessary conditions for the problem in a different light, but is equivalent to the method presented here.) In actuality, all combinations of control surface pairs at their position limits must be evaluated.

Begin by considering the following moment equations for the 1–2 pair:

$$L_{12} = K_l(\delta_1 - \delta_2) \tag{12}$$

$$M_{12} = K_m(\delta_1 + \delta_2) \tag{13}$$

$$N_{12} = K_n\left(\delta_1^2 - \delta_2^2\right) \tag{14}$$

where K_l, K_m, and K_n are the rolling, pitching, and yawing control derivatives, respectively, and are as defined earlier. Eliminating the parameter δ_1, we can write the pitching and yawing moments as functions of the rolling moment,

$$M_{12}(L_{12}) = K_m(2\delta_2 + L_{12}/K_l) \tag{15}$$

$$N_{12}(L_{12}) = K_n\left(L_{12}^2 / K_l^2\right) + 2\delta_2(L_{12}/K_l) \tag{16}$$

Repeating the process for the 3–4 effector pair to eliminate δ_3 subsequently yields

$$M_{34}(L_{34}) = C_m(2\delta_4 + L_{34}/C_l) \tag{17}$$

$$N_{34}(L_{34}) = C_n\left[L_{34}^2 / C_l^2 + 2\delta_4(L_{34}/C_l)\right] \tag{18}$$

where C_l, C_m, and C_n are the rolling, pitching, and yawing control derivatives, respectively, defined earlier.

To compute the AMS boundary, we will assume that all feasible ordered pairs (L, M) can be computed a priori. Note that when this approach is implemented in a flight control system this does not impose any kind of restriction because we assume that we are able to determine the feasibility of a given (L, M). We fix L and M at some arbitrary value and let $L_{34} = L - \bar{L}$, where $\bar{L}$ is the attaching point. (The choice of notation here is to be consistent with that given in Ref. 10.) The equations for the pitching and yawing moments then become

$$M = K_m(2\,\delta_2 + \bar{L}/K_l) + C_m[2\,\delta_4 + (L - \bar{L})/C_l] \tag{19}$$

$$N = K_n\left[\bar{L}^2 / K_l^2 + 2(\bar{L}\delta_2/K_l)\right] + C_n\left\{(L-\bar{L})^2 / C_l^2 + 2[(L-\bar{L})\delta_4/C_l]\right\} \tag{20}$$

If we were not concerned with the pitching moment, we would simply apply the theorem, differentiate Eq. (20), and solve for the attaching point $\bar{L}$, as was done in the two-dimensional case. We are including an additional equation for the pitching moment to account for the third control axis; therefore, an alternate approach is necessary. To determine the AMS boundary for a given point (L, M), a constrained optimization problem mustbe posed and solved. Therefore, we consider the following optimization problem:

$$\min J = K_n\left[\bar{L}^2\big/K_l^2 + 2(\bar{L}\delta_2/K_l)\right] + C_n\left\{(L-\bar{L})^2\big/C_l^2 + 2[(L-\bar{L})\delta_4/C_l]\right\} \tag{21}$$

subject to

$$M = K_m(2\delta_2 + \bar{L}/K_l) + C_m[2\delta_4 + (L-\bar{L})/C_l] \tag{22}$$

$$\underline{\delta}_2 \le \delta_2 \le \bar{\delta}_2 \tag{23}$$

$$\underline{\delta}_4 \le \delta_4 \le \bar{\delta}_4 \tag{24}$$

The effect of considering all three axes is that we must now solve an optimization problem with a single equality constraint and four inequality constraints to find the boundary that encloses the AMS. By including the inequality constraints for control effectors, we no longer have to carry along Remarks 1 and 2 because they are now accounted for in the objective function. We form the following Lagrangian for the preceding optimization problem:

$$\begin{aligned}\mathcal{L} = {} & K_n\left[\bar{L}^2\big/K_l^2 + 2(\bar{L}\delta_2/K_l)\right] + C_n\left\{(L-\bar{L})^2\big/C_l^2 \right.\\ & \left. + 2[(L-\bar{L})\delta_4/C_l]\right\} - \lambda\{M - K_m(2\delta_2 + \bar{L}/K_l) \\ & - C_m[2\delta_4 + (L-\bar{L})/C_l]\} - \mu_1(\bar{\delta}_2 - \delta_2) - \mu_2(\delta_2 - \underline{\delta}_2) \\ & - \mu_3(\bar{\delta}_4 - \delta_4) - \mu_4(\delta_4 - \underline{\delta}_4)\end{aligned} \tag{25}$$

Differentiating the Lagrangian with respect to $\bar{L}$, δ_2, δ_4, and λ gives the first-order necessary conditions:

$$\frac{\partial\mathcal{L}}{\partial\bar{L}} = 2\frac{K_n}{K_l^2}(\bar{L} + K_l\delta_2) + 2\frac{C_n}{C_l^2}(L - \bar{L} + C_l\delta_4) - \lambda\left(\frac{C_m}{C_l} - \frac{K_m}{K_l}\right) \tag{26}$$

$$\frac{\partial\mathcal{L}}{\partial\delta_2} = 2\frac{K_n}{K_l}\bar{L} + 2\lambda K_m + \mu_1 - \mu_2 \tag{27}$$

$$\frac{\partial\mathcal{L}}{\partial\delta_4} = 2\frac{C_n}{C_l}(L - \bar{L}) + 2\lambda C_m + \mu_3 - \mu_4 \tag{28}$$

$$\frac{\partial\mathcal{L}}{\partial\lambda} = M - K_m\left(2\delta_2 + \frac{\bar{L}}{K_l}\right) - C_m\left(2\delta_4 + \frac{L-\bar{L}}{C_l}\right) \tag{29}$$

Setting Eqs. (26–29) equal to zero and solving for $\bar{L}$, δ_2, δ_4, and λ yields

$$\bar{L} = \frac{K_l[2C_nK_mL + C_lK_m(\mu_3 - \mu_4)]}{2(C_nK_lK_m + C_lC_mK_n)} \tag{30}$$

$$- \frac{K_lC_lC_m(\mu_1 - \mu_2)}{2(C_nK_lK_m + C_lC_mK_n)} \tag{31}$$

$$\delta_2 = \frac{2C_n(K_lM - K_mL) - C_mK_l(\mu_3 - \mu_4)}{4(C_nK_lK_m + C_lC_mK_n)} + \frac{C_l[2C_m(\mu_1 - \mu_2) - K_m(\mu_3 - \mu_4)]}{4(C_nK_lK_m + C_lC_mK_n)} \tag{32}$$

$$\delta_4 = \frac{C_l[2K_nM - K_m(\mu_1 - \mu_2)] - 2C_mK_nL}{4(C_nK_lK_m + C_lC_mK_n)} + \frac{K_l[2K_m(\mu_3 - \mu_4) - C_m(\mu_1 - \mu_2)]}{4(C_nK_lK_m + C_lC_mK_n)} \tag{33}$$

$$\lambda = -\frac{C_n[2K_nL + K_l(\mu_1 - \mu_2)]}{2(C_nK_lK_m + C_lC_mK_n)} + \frac{C_lK_n(\mu_3 - \mu_4)}{2(C_nK_lK_m + C_lC_mK_n)} \tag{34}$$

When solving the optimization problem, we must also include the following equality and inequality constraints:

$$\mu_1(\bar{\delta}_2 - \delta_2) = 0 \tag{35}$$

$$\mu_2(\delta_2 - \underline{\delta}_2) = 0 \tag{36}$$

$$\mu_3(\bar{\delta}_4 - \delta_4) = 0 \tag{37}$$

$$\mu_4(\delta_4 - \underline{\delta}_4) = 0 \tag{38}$$

$$\mu_1, \mu_2, \mu_3, \mu_4 \ge 0 \tag{39}$$

According to optimization theory, the value of the yawing moment that optimizes Eq. (25) must satisfy the Kuhn–Tucker necessary conditions (see Ref. 13). Therefore, we must evaluate the Kuhn–Tucker points that result from the enumeration of all possible combinations of δ_2 and δ_4 set at their upper and lower bounds taken one at a time and two at a time. This will result in eight different Kuhn–Tucker points to consider. For the case where we have four control effectors, we will have 32 Kuhn–Tucker points to evaluate. In fact, these Kuhn–Tucker points correspond to the set of control effector combinations as determined by swept volume theory. Once all of the Kuhn–Tucker points are constructed, the feasibility of a candidate Kuhn–Tucker point is checked. Feasibility is achieved when the appropriate inequality and equality constraints are satisfied. All combinations of surfaces set at their upper and lower limits are searched for feasible Kuhn–Tucker points for the given values of L and M. Feasible Kuhn–Tucker points are kept in a list, and once the list is completed, then the minimum (or maximum) value of N and the corresponding control surface deflections can easily be found using a simple search. It is the maximum and minimum values of N that define the AMS boundary. Note that it is possible for there to be multiple sets of control surface deflections that will produce the same point on the boundary.

Next we present an example where we find the minimum and maximum yawing moments given a feasible (L, M). The control derivatives have the following values: $K_l = -4610$ ft · lb/deg, $K_m = -2489$ ft · lb/deg, $K_n = -34$ ft · lb/deg^2, $C_l = K_l/2$, $C_m = K_m$, and $C_n = K_n/4$. The limits on the control effectors are $-30 \le \delta_i \le 30$ deg, $i = 1, 2, 3, 4$. If we fix $L = M = 0$, we find two minima with a value of −22,950 ft · lb. Physically, this implies that there are two different combinations of control surface deflections that will produce the minimum yawing moments while satisfying the constraints on the pitching and rolling moments. The control surface deflections corresponding to these minima are $\delta_1 = 22.5$, $\delta_2 = 7.5$, $\delta_3 = -30$, and $\delta_4 = 0$ deg and $\delta_1 = -22.5$, $\delta_2 = -7.5$, $\delta_3 = 30$, and $\delta_4 = 0$ deg. To find the maxima for a given (L, M), one will simply follow the outlined procedure. The only difference is that one uses $-N$ in Eq. (25). At the point $L = 0$, $M = 0$, we find two maxima where $N = 22{,}950$ ft · lb.

The utility of this method is shown in Fig. 6, where the AMS is shown over the range of rolling moment with pitching moment fixed to be zero. To compute the AMS, one simply iterates over all feasible values of L and M and then applies the Kuhn–Tucker conditions to determine the maximum and minimum values of yawing moment for each ordered pair. This approach, although it requires an exhaustive search of all possible Kuhn–Tucker points for a given L and M, provides an accurate estimation of the AMS.

The composite AMS is shown in Fig. 7. As a comparison, Fig. 8 shows the AMS generated by a linear approximation. Note, first, the difference in the shapes of the two sets. The linear AMS predicts the correct projection onto the L–M plane, but the yawing moment is either over- or underestimated or has the incorrect sign. The nonlinear AMS provides a much more accurate representation of the aircraft's control authority.

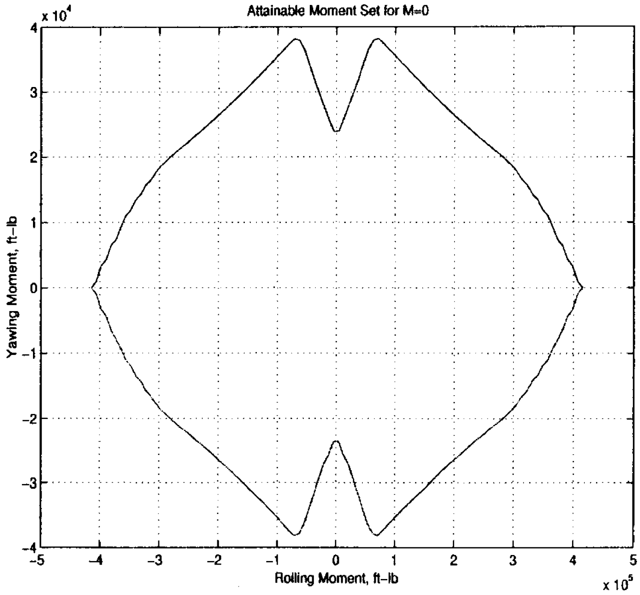

Fig. 6 Achievable yawing moments for $M = 0$.

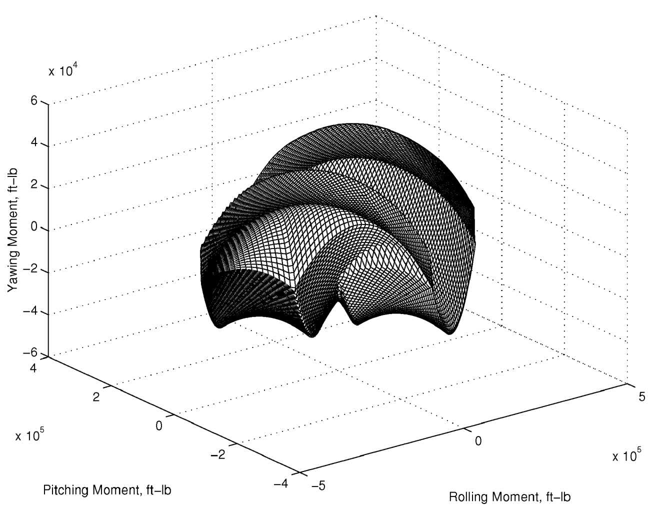

Fig. 7 Nonlinear attainable moment set.

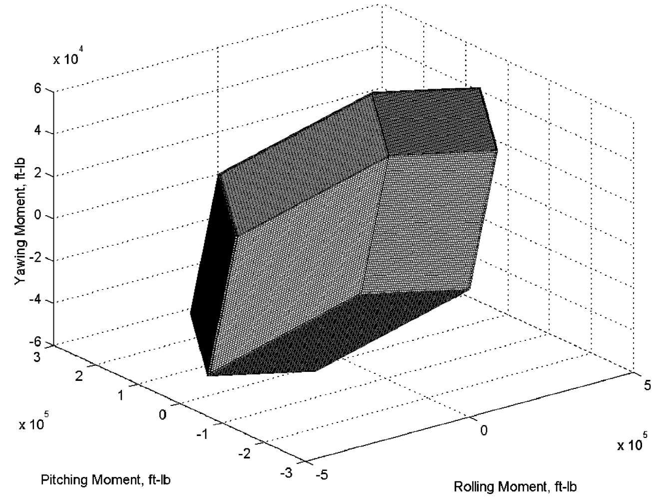

Fig. 8 Linear attainable moment set.

Flight Control System Implementation

Given that the nonlinear AMS can now be constructed, the question remains on how to utilize the AMS in an actual flight control system. Given that state-of-the-art digital flight control systems operate with update rates between 50 and 100 Hz, it is necessary to have an efficient method that allows the control allocation problem to be solved in real time. In this section, we address this question and propose two methods for using the AMS to solve the nonlinear control allocation problem.

As proposed by Durham,[6] the AMS is to be used in a direct allocation approach to control allocation in the following manner: Given the vector $\boldsymbol{d}_{\text{des}} = [L_{\text{des}} \quad M_{\text{des}} \quad N_{\text{des}}]^T$, where L_{des}, M_{des}, and N_{des} are the desired rolling, pitching, and yawing moments, respectively, determine the attainable moment with the largest magnitude that is collinear with $\boldsymbol{d}_{\text{des}}$. Once this vector is obtained, one can check the command feasibility and ultimately determine the control effector positions.

There are two ways to approach the problem of determining the maximum attainable moment. The first approach is to construct the entire AMS off-line and then store it in some manner that allows it to be efficiently called at each update of the flight control system. Once the AMS is retrieved, some numerical method is employed to determine the intersection of a vector that is collinear with $\boldsymbol{d}_{\text{des}}$ and the AMS. The downside to this approach is that an AMS is required at multiple flight conditions for the nominal, unfailed configuration. In addition, it is necessary to analyze all likely failure cases over some set of flight conditions and then construct an AMS for these configurations too.

A second approach avoids the computation of the entire AMS and is a more likely candidate for implementation. This approach is predicated on the ability to first determine the feasibility of a reduced desired moment $\hat{\boldsymbol{d}}_{\text{des}} = [L_{\text{des}} \quad M_{\text{des}} \quad 0]^T$. To check for feasibility of this reduced vector, one could apply Durham's method[7] for moments that are linear in the controls. A second approach that is more general, and will work for both linear and nonlinear controls, relies on the fact that a line in moment space and coincident with the desired moment, when projected on the roll–pitch plane, can be written as

$$L_{\text{des}} \sum_{i=1}^{n} M(\delta_i) - M_{\text{des}} \sum_{i=1}^{n} L(\delta_i) = 0 \tag{40}$$

where n is the number of control effectors. Because the AMS boundary in the plane occurs when $n - 1$ effectors are set to their limits, we are able to solve this equation for the remaining control effector position. The difficulty with this approach is that Eq. (40) must be solved for $n\,2^{n-1}$ combinations of the controls. Therefore, given a large number of controls, an exhaustive search becomes impractical. Also, for nonlinear equations that are not low-order polynomial functions a numerical root-finding technique is necessary to solve for the remaining effector position. In addition, this approach can admit multiple feasible solutions to each root-finding problem, that is, within the upper and lower bounds of the control surfaces.

Once the feasibility of the reduced vector has been determined, we have to determine the feasibility of N_{des}. For a feasible reduced moment command, the Kuhn–Tucker test is applied to determine the maximum and minimum yawing moments given L_{des} and M_{des}. It is then possible to determine whether $\boldsymbol{d}_{\text{des}}$ is feasible by simply checking the elevation of $\boldsymbol{d}_{\text{des}}$ above the roll–pitch plane and comparing this angle with the maximum or minimum N given L_{des} and M_{des}. If the commanded moment is indeed feasible, then the following nonlinear, constrained optimization problem is solved:

$$\min_{\boldsymbol{\delta}} \|\boldsymbol{\delta} - \boldsymbol{\delta}_p\|_2^2 \tag{41}$$

subject to

$$\tfrac{1}{2}[L_{\text{des}} - L(\boldsymbol{\delta})]^2 + \tfrac{1}{2}[M_{\text{des}} - M(\boldsymbol{\delta})]^2 + \tfrac{1}{2}[N_{\text{des}} - N(\boldsymbol{\delta})]^2 = 0 \tag{42}$$

where $\boldsymbol{\delta}_p$ is a vector of preferred effector positions. Because the commanded moment has been determined to be feasible, a solution to this optimization problem is guaranteed to exist. However, if it is determined that N_{des} is infeasible or if the reduced moment command is infeasible, we must clip the desired moment to the

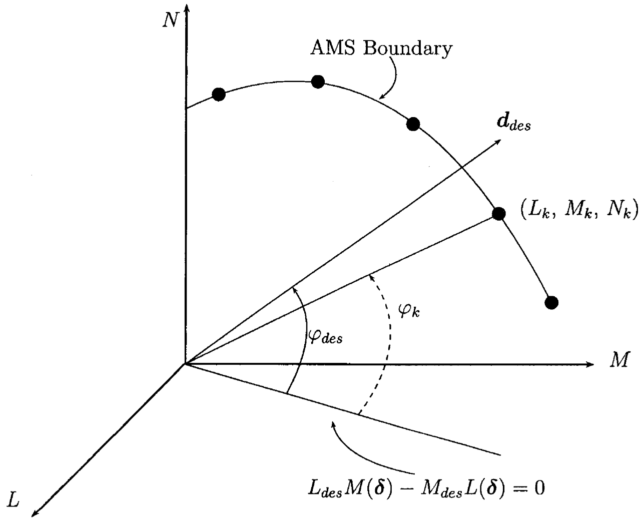

Fig. 9 Technique for clipping to AMS boundary.

AMS boundary while preserving the direction of $\boldsymbol{d}_{\text{des}}$ in moment space.

To clip $\boldsymbol{d}_{\text{des}}$ to the AMS boundary when the ordered pair $(L_{\text{des}}, M_{\text{des}})$ is deemed feasible, we select a finite set of ordered pairs (L_k, M_k) that are in the domain $[0, L_{\text{des}}] \times [0, M_{\text{des}}]$ and that also satisfies Eq. (40). However, if $(L_{\text{des}}, M_{\text{des}})$ is not feasible, we select (L_k, M_k) that satisfy Eq. (40), but lie in the domain $[0, L_b] \times [0, M_b]$, where L_b is the clipped rolling moment and M_b is the clipped pitching moment. In either case, the Kuhn–Tucker test is applied at each ordered pair (L_k, M_k) to determine the maximum or minimum yawing moments, as appropriate, and the associated control effector displacements. We now have a simple, discrete representation of the AMS boundary in the correct octant along with the associated control effector positions that determine the AMS boundary (Fig. 9). Furthermore, for each ordered triplet (L_k, M_k, N_k), we determine the angle φ_k between the vector $[L_k\ M_k\ N_k]^T$ and the roll–pitch plane. To find the value of N that will preserve the elevation of the moment command, φ_{des}, above the roll–pitch plane, one can simply perform a cubic spline interpolation of $N(\varphi_k)$ given φ_{des}. The control effector positions may then be estimated by interpolation.

Conclusions

A method for the determination of the attainable moment set for a class of multiple nonlinear control effectors was presented. The method extends previous work that was done on the generation of the nonlinear attainable moment set boundary in the planar case to the three-dimensional case and was illustrated by considering single and multiple LR control effector pairs. Swept volume theory can be used to determine the set of candidate surfaces for the boundary of the attainable moment set. However, the boundary itself cannot be easily determined from these surfaces. Instead, the determination of the attainable moment set boundary was posed as a nonlinear, constrained optimization problem. For a point to be an AMS boundary candidate, the Kuhn–Tucker first-order necessary conditions must be satisfied. An algorithm was developed where the Kuhn–Tucker points for a given point in the pitch–roll plane are constructed for each control effector configuration that generates a candidate boundary point. The Kuhn–Tucker conditions for every combination of the control effector positions are then checked for feasibility, and the points on the boundary are those that produce extremal values of the objective function. Within a flight control system, it was shown how the nonlinear attainable moment set boundary can be used to determine feasibility of moment commands generated by the flight control system. If a moment command is deemed to be infeasible, the command is clipped to the boundary of the attainable moment set. If the commanded moment is feasible, a constrained optimization problem is then solved to drive the control surface deflections to some preferred values.

Appendix A: Alternate Approach for the Determination of AMS

We present an alternate approach for the determination of the sweep boundary. The approach remains, given L and M, to evaluate the Kuhn–Tucker points for all possible combinations of the control surfaces, taken in pairs, and set at their upper and lower limits. The difference between this approach and the one that we present earlier is that rolling moment as a function of control effector position now explicitly appears in the optimization problem. This approach, which is equivalent to the approach presented earlier, is more general because, with this particular problem formulation, it is easier to handle aircraft that have a larger number of control surfaces than what was considered earlier. The boundary determination problem is then posed as follows:

$$\min N = K_n\left(\delta_1^2 - \delta_2^2\right) + C_n\left(\delta_3^2 - \delta_4^2\right) \tag{A1}$$

subject to

$$\begin{aligned} L &= K_l(\delta_1 - \delta_2) + C_l(\delta_3 - \delta_4) \\ M &= K_m(\delta_1 + \delta_2) + C_m(\delta_3 - \delta_4) \\ &\underline{\delta}_i \le \delta_i \le \bar{\delta}_i, \qquad i = 1, 2, 3, 4 \end{aligned} \tag{A2}$$

The Lagrangian then becomes

$$\begin{aligned} \mathscr{L} = {} & K_n\left(\delta_1^2 - \delta_2^2\right) + C_n\left(\delta_3^2 - \delta_4^2\right) - \lambda_1(L - K_l(\delta_1 - \delta_2) \\ & - C_l(\delta_3 - \delta_4)) - \lambda_2(M - K_m(\delta_1 + \delta_2) - C_m(\delta_3 - \delta_4)) \\ & - \mu_1(\bar{\delta}_1 - \delta_1) - \mu_2(\delta_1 - \underline{\delta}_1) - \mu_3(\bar{\delta}_2 - \delta_2) - \mu_4(\delta_2 - \underline{\delta}_2) \\ & - \mu_5(\bar{\delta}_3 - \delta_3) - \mu_6(\delta_3 - \underline{\delta}_3) - \mu_7(\bar{\delta}_4 - \delta_4) - \mu_8(\delta_4 - \underline{\delta}_4) \end{aligned} \tag{A3}$$

The first-order necessary conditions are

$$\frac{\partial \mathscr{L}}{\partial \delta_1} = 2K_n\delta_1 + \lambda_1 K_l + \lambda_2 K_m + \mu_1 - \mu_2 = 0 \tag{A4}$$

$$\frac{\partial \mathscr{L}}{\partial \delta_2} = -2K_n\delta_2 - \lambda_1 K_l + \lambda_2 K_m + \mu_3 - \mu_4 = 0 \tag{A5}$$

$$\frac{\partial \mathscr{L}}{\partial \delta_3} = 2C_n\delta_3 + \lambda_1 C_l + \lambda_2 C_m + \mu_5 - \mu_6 = 0 \tag{A6}$$

$$\frac{\partial \mathscr{L}}{\partial \delta_4} = -2C_n\delta_4 - \lambda_1 C_l + \lambda_2 C_m + \mu_7 - \mu_8 = 0 \tag{A7}$$

$$\frac{\partial \mathscr{L}}{\partial \lambda_1} = L - K_l(\delta_1 - \delta_2) - C_l(\delta_3 - \delta_4) = 0 \tag{A8}$$

$$\frac{\partial \mathscr{L}}{\partial \lambda_2} = M - K_m(\delta_1 + \delta_2) - C_m(\delta_3 - \delta_4) = 0 \tag{A9}$$

subject to the following equality and inequality constraints:

$$\mu_1(\bar{\delta}_1 - \delta_1) = 0 \tag{A10}$$

$$\mu_2(\delta_1 - \underline{\delta}_1) = 0 \tag{A11}$$

$$\mu_3(\bar{\delta}_2 - \delta_2) = 0 \tag{A12}$$

$$\mu_4(\delta_2 - \underline{\delta}_2) = 0 \tag{A13}$$

$$\mu_5(\bar{\delta}_3 - \delta_3) = 0 \tag{A14}$$

$$\mu_6(\delta_3 - \underline{\delta}_3) = 0 \tag{A15}$$

$$\mu_7(\bar{\delta}_4 - \delta_4) = 0 \tag{A16}$$

$$\mu_8(\delta_4 - \underline{\delta}_4) = 0 \tag{A17}$$

$$\mu_1, \mu_2, \mu_3, \mu_4, \mu_5, \mu_6, \mu_7, \mu_8 \ge 0 \tag{A18}$$

Once the first-order necessary conditions are determined, we follow the same procedure as presented earlier. Subsequently, we take every combination of control surface deflections at their extremal values such that the preceding inequalities and equalities in μ_i are satisfied. The Kuhn–Tucker points are computed for each combination. Finally, a search is conducted over the feasible Kuhn–Tucker points for each (L, M) ordered pair to find the control surface deflections and the yawing moment that optimizes the objective function.

Appendix B: Nonlinear Programming Formulation of Direct Allocation

An alternate approach to the direct allocation method outlined in Appendix A is to solve an equivalent nonlinear programming problem. This problem formulation follows from Bodson,[3] who gives a linear programming formulation of the direct allocation problem for control moments that are linear functions of the control effectors. The formulation for the nonlinear programming problem is as follows:

$$\min J = -\boldsymbol{d}_{\text{des}}^T \begin{bmatrix} L(\boldsymbol{\delta}) \\ M(\boldsymbol{\delta}) \\ N(\boldsymbol{\delta}) \end{bmatrix} \tag{B1}$$

subject to

$$L_{\text{des}} M(\boldsymbol{\delta}) - M_{\text{des}} L(\boldsymbol{\delta}) = 0 \tag{B2}$$

$$L_{\text{des}} N(\boldsymbol{\delta}) - N_{\text{des}} L(\boldsymbol{\delta}) = 0 \tag{B3}$$

$$\boldsymbol{\delta}_{\min} \leq \boldsymbol{\delta} \leq \boldsymbol{\delta} \tag{B4}$$

where $\boldsymbol{d}_{\text{des}} = [L_{\text{des}}\ M_{\text{des}}\ N_{\text{des}}]^T$ is the desired moment command, L is the rolling moment, M is the pitching moment, and N is the yawing moment. The bounds on the controls $\boldsymbol{\delta}$ are given by $\boldsymbol{\delta}_{\min}$ and $\boldsymbol{\delta}_{\max}$. At each frame update of the flight control system, we solve the preceding nonlinear programming problem for the controls. To determine feasibility of $\boldsymbol{d}_{\text{des}}$, we compute the parameter ρ defined as

$$\rho = -J \Big/ \|\boldsymbol{d}_{\text{des}}\|_2^2 \tag{B5}$$

If $\rho \leq 1$, then we stop because the moment command is either infeasible or is on the AMS boundary and $\boldsymbol{\delta}$ corresponds to the clipped moment on the AMS boundary. On the other hand, if $\rho > 1$, the commanded moment is feasible; therefore, we need to determine the control effector positions that will give the desired moment. In the linear case, one simply needs to scale the controls by ρ; however, in the case where the moments are nonlinear functions of the controls, it is necessary to solve a second optimization problem. The optimization problem is defined as

$$\min_{\delta} \|\boldsymbol{\delta} - \boldsymbol{\delta}_p\|_2^2 \tag{B6}$$

subject to

$$\tfrac{1}{2}[L_{\text{des}} - L(\boldsymbol{\delta})]^2 + \tfrac{1}{2}[M_{\text{des}} - M(\boldsymbol{\delta})]^2 + \tfrac{1}{2}[N_{\text{des}} - N(\boldsymbol{\delta})]^2 = 0 \tag{B7}$$

The solution to this problem will minimize the control surface deflections relative to some preferred deflections while preserving the direction of a feasible desired moment command. Because the commanded moment has been determined to be feasible, a solution to this optimization problem is guaranteed to exist.

Acknowledgments

This work was performed while the first author held a National Research Council Research Associateship Award at the U.S. Air Force Research Laboratory.

A previous version of this paper was presented at the 2003 Institute of Electrical and Electronics Engineers Aerospace Conference, Big Sky, Montana.

References

[1]Doman, D., and Ngo, A., "Dynamic Inversion-Based Adaptive/Reconfigurable Control of the X-33 on Ascent," *Journal of Guidance, Control, and Dynamics*, Vol. 25, No. 2, 2002, pp. 275–284.

[2]Buffington, J., "Modular Control Law Design for the Innovative Control Effectors (ICE) Tailless Fighter Aircraft Configuration 101-3," U.S. Air Force Research Lab.,Technical Rept. AFRL-VA-WP-TR 1999-3057, Wright–Patterson AFB, OH, June 1999.

[3]Bodson, M., "Evaluation of Optimization Methods for Control Allocation," *Journal of Guidance, Control, and Dynamics*, Vol. 25, No. 4, 2002, pp. 703–711.

[4]Page, A., and Steinberg, M., "A Closed-Loop Comparison of Control Allocation Methods," AIAA Paper 2000-4538, Aug. 2000.

[5]Page, A., and Steinberg, M., "High-Fidelity Simulation Testing of Control Allocation Methods," AIAA Paper 2002-4547, Aug. 2002.

[6]Durham, W., "Attainable Moments for the Constrained Control Allocation Problem," *Journal of Guidance, Control, and Dynamics*, Vol. 17, No. 6, 1994, pp. 1371–1373.

[7]Durham, W., "Constrained Control Allocation: Three-Moment Problem," *Journal of Guidance, Control, and Dynamics*, Vol. 17, No. 2, 1994, pp. 330–336.

[8]Abdel-Malek, K., and Yeh, H., "Geometric Representation of the Swept Volume Using Jacobian Rank Deficiency Conditions," *Computer-Aided Design*, Vol. 29, No. 6, 1997, pp. 457–468.

[9]Abdel-Malek, K., and Yeh, H., and Othman, S., "Swept Volumes: Void and Boundary Identification," *Computer-Aided Design*, Vol. 30, No. 13, 1998, pp. 1009–1018.

[10]Doman, D., and Sparks, A., "Concepts for Constrained Control Allocation of Mixed Quadratic and Linear Effectors," American Automatic Control Council, Paper ACC02-AIAA1028, May 2002.

[11]Bolender, M., and Doman, D., "A Method for the Determination of the Attainable Moment Set for Non-Linear Control Effectors," *Proceedings of the 2003 IEEE Aerospace Conference*, [CD ROM], Inst. of Electrical and Electronics Engineers, New York, 2003.

[12]Abdel-Malek, K., Blackmore, D., and Joy, K., "Swept Volumes: Foundations, Perspectives, and Applications," URL: http://www.engineering.uiowa.edu/∼amalek/papers/swept-volume-review.pdf [cited 4 May 2004].

[13]Reklaitis, G., Ravindran, A., and Ragsdell, K., *Engineering Optimization: Methods and Application*, Wiley-Interscience, New York, 1983, pp. 195–200.